Chemical Engineering Journal 394 (2020) 124957

Contents lists available at ScienceDirect

Chemical Engineering Journal

journal homepage: www.elsevier.com/locate/cej

Upgrading biogas with novel composite carbon molecular sieve (CCMS) membranes: Experimental and techno-economic assessment

J.A. Medrano[a], M.A. Llosa-Tanco[b], V. Cechetto[a], D.A. Pacheco-Tanaka[b], F. Gallucci[a,*]

[a] Inorganic Membranes and Membrane Reactors, Sustainable Process Engineering, Department of Chemical Engineering and Chemistry, Eindhoven University of Technology, De Rondom 70, 5612 AP Eindhoven, The Netherlands

[b] TECNALIA, Energy and Environment Division. Mikeletegi Pasealekua 2, 20009 San Sebastián-Donostia, Spain

HIGHLIGHTS

- Carbon membranes have been investigated experimentally for biogas upgrading.
- The performance of carbon membranes exceeds the Robeson limit of polymeric membranes.
- The economics of biogas upgrading with carbon membranes have been evaluated.
- Carbon membranes can be installed in existing reforming plants for H_2 production.
- 95% of carbon emissions can be avoided by using biogas for H_2 production.

GRAPHICAL ABSTRACT

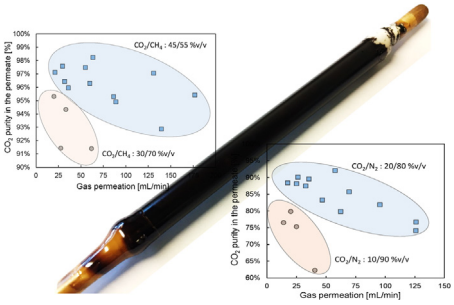

ARTICLE INFO

Keywords:
Biogas upgrading
Climate change
Carbon membranes
Techno-economics

ABSTRACT

The use of biogas as feedstock for hydrogen production was widely proposed in the literature in the last years as a strategy to reduce anthropogenic carbon emissions. However, its lower heating value compared to natural gas hampers the revamping of existing reforming plants. The use of composite carbon molecular sieve membranes for biogas upgrading (CO_2 removal from biogas) was investigated experimentally in this work. In particular, ideal perm-selectivities and permeabilities above the Robeson plot for CO_2/CH_4 mixtures have been obtained. These membranes show better performances compared to polymeric membranes, which are nowadays commercialized for CO_2 separation in natural gas streams. Compared to polymeric membranes, carbon membranes do not show deactivation by plasticization when exposed to CO_2, and thus can find industrial application. This work was extended with a techno-economic analysis where carbon membranes are installed in a steam methane reforming plant. Results have been first validated with data from literature and show that the use of biogas increases the costs of hydrogen production to a value of 0.25 €/Nm^3 compared to the benchmark technology (0.21 €/Nm^3). On the other hand, the use of biogas leads to a decrease in carbon emissions up to 95%, thus the use of biogas for hydrogen production is foreseen as a very interesting alternative to conventional technologies in view of the reduction in the carbon footprint in the novel technologies that are to be installed in the near future.

* Corresponding author.
E-mail address: f.gallucci@tue.nl (F. Gallucci).

https://doi.org/10.1016/j.cej.2020.124957
Received 13 February 2020; Received in revised form 31 March 2020; Accepted 2 April 2020
Available online 06 April 2020

Nomenclature

Acronyms and abbreviations

BEC	Bare Erected Cost
C&OC	Contingencies and owner's costs
CCF	Capital charge factor
CCGT	Combined Cycle Gas Turbine
CCS	Carbon Capture and Storage
CMSM	Carbon Molecular Sieve Membranes
COH	Cost of Hydrogen
EPC	Engineering procurement and construction
IC	Indirect Costs
IEA	International Energy Agency
IPPC	Intergovernmental Panel on Climate Change
MMM	Mixed Matrix Membranes
MOFs	Metal Organic Framework
NETL	National Energy Technology Laboratory
O&M	Operation and maintenance
PSA	Pressure Swing Adsorption
S/C	Steam to Carbon ratio
TDPC	Total Direct Plant Costs
TIC	Total Installation Costs
TOC	Total overnight Costs
WGS	Water Gas Shift

Symbols and units

C_0	Reference cost (M€)
E_a	Activation energy (kJ/mol)
E_{CO2}	CO_2 emissions (kg/s)
$E_{CO2,eq}$	Equivalent CO_2 emissions (kg/s)
$h_{liqsar@6bar}$	Enthalpy of liquid at saturation point at 6 bar (MJ/kg)
$h_{steam@6bar}$	Enthalpy of steam at 6 bar (MJ/kg)
J_i	Permeance (mol/s/m^2/Pa)
LHV_{NG}	Lower heating value of natural gas (kJ/kg)
$\dot{m}_i$	Mas flow of component i (kg/s)
$\dot{m}_{i,eq}$	Equivalent mass flow of component i (kg/s)
P_0	Permeability (mol/s/m/Pa)
Q_{th}	Thermal heat (MW)
R	Ideal gas constant (J/K/mol)
S_0	Reference capacity
t	membrane thickness (m)
T	Temperature (K)
W_{el}	electric power (MW)
Δp_i	Pressure difference of component i (Pa)
$\eta_{el,ref}$	yield for power production
η_{H2}	H_2 production efficiency
$\eta_{H2,eq}$	Equivalent H_2 production efficiency
$\eta_{th,ref}$	yield for thermal power production

1. Introduction

Since the industrial revolution, the CO_2 concentration in the atmosphere has experienced a continuous increase associated to the extensive use of fossil fuel resources for power generation, and many of the observed changes in the climate are consequence of these greenhouse gases emissions. The agreement signed in Paris (December 2015) against climate changes proposes the reduction in CO_2 emissions to the atmosphere in order to restrict the increase in atmospheric temperature to below 2 °C by 2100. The most realistic scenario requires a reduction of around 40–70% of anthropogenic emissions by 2050 and near-zero emissions by 2100 [1].

Nowadays, different strategies have been proposed for reducing these emissions as summarized by the Intergovernmental Panel on Climate Change (IPPC) [2] in collaboration with the International Energy Agency (IEA) [3]. In the long-term, the preferred one consists in the complete substitution of current technologies powered by fossil fuels with the use of renewable sources. Among the different renewable sources, biogas has the potential to take over the role of natural gas as fuel source. Biogas can be obtained by anaerobic digestion of organic wastes and is a gas mixture containing mainly methane (50–70 %vol.), carbon dioxide (30–40 %vol.), and small quantities of other gases such as H_2, H_2S or N_2 [4,5]. The biogas, once cleaned, can be used directly in gas engines and gas turbines to produce electricity, and the net carbon emissions can be assumed zero since the CO_2 was previously adsorbed by the natural waste (viz. agricultural plants, fruit, etc.) [6]. However, the overall conversion efficiency of this biofuel into electricity is about 10–16%. This efficiency is rather low as compared to the efficiency achieved with natural gas for electricity generation, which is normally in the range of 39% for large gas turbines and up to 58% in Combined Cycle Gas Turbine processes (CCGT) [7,8]. This is associated to the much lower energy content in the biogas, which could be around 20–60% of the lower heating value of a natural gas feedstock depending on the concentration of CH_4.

Biogas could also be used for H_2 production, largely consumed in the ammonia and methanol production processes, and foreseen as a perfect energy carrier because of its high energy density and the fact that in its combustion the only product is steam. H_2 can be produced from biogas through dry reforming, which is a highly endothermic reaction that produces a syngas with a molar ration H_2/CO of 1 [9,10]. This process is normally followed by water gas shift reaction to maximize the H_2 yield. However, it is not commonly used at industrial level due to the high coke formation and the low H_2/CO ratio produced [11]. Instead, nowadays there is an increased interest in the production of bio-methane by upgrading the biogas by removing the CO_2, H_2S and water vapor [6,12,13]. The use of bio-methane is preferred over the biogas since the energy density of the fuel source is increased and it can be used directly in all existing and installed plants and can also be sent into the natural gas grid. Biogas upgrading can be carried out by means of different techniques depending on the bio-methane quality required and the biogas composition. Several technologies are nowadays commercially available for full scale upgrading of biogas. In particular, Pressure Swing Adsorption (PSA), Absorption (scrubbing) and Membranes.

In PSA, CO_2 is separated at elevated pressures by its adsorption on activated carbon or zeolites. In this technology it is important to clean the biogas before feeding it into the PSA unit since H_2S would be adsorbed irreversibly on the adsorbent material and water can damage its surface [14]. Nowadays, there are commercially available PSA units that release a fuel source with a minimum concentration of CH_4 of 96%. However, the costs of this technology strongly depends on the electricity prices, since it requires continuous compression and expansion [5].

Scrubbing is another typical technology implemented at industrial scale. The absorption technology is based on three different approaches: water scrubbing, organic scrubbing and chemical scrubbing. Only in the case of chemical scrubbing there is need of pre-cleaning of the biogas, although it operates at lower pressures with a corresponding decrease in electrical consumption. The methane purity that can be achieved with these technologies is rather high (> 96%) and it is installed for large-scale upgrading capacities. In the case of chemical scrubbing (normally with amines) the purity of the bio-methane can be > 99%, although it demands available heat in the plant.

Membranes are only installed at industrial scale in low capacity plants. This technology is also very attractive for large scale upgrading plants since the separation mechanism is the simplest. These

membranes are typically polymer hollow fibers permeable to carbon dioxide, water and ammonia, and in a minor extent to methane and nitrogen. However, polymeric membranes have reached an upper bound limit (summarized by Robeson [15]), with a compromise between CO_2 fluxes and CO_2/CH_4 separation (perm-selectivity) [16]. Furthermore, in presence of high CO_2 concentrations they suffer from plasticization and swelling, and their lifetime is thus reduced. This fact has limited their use at industrial scale. Moreover, in order to achieve the desired bio-methane purities (and minimize the losses), several membrane stages are required. In a single step the removal of CO_2 leads to CH_4 concentrations below 92%, and inter-stage compressors are needed in order to increase the feed pressure with a concomitant increase in capital and operational expenses.

Since membrane technology can largely reduce the upgrading costs, research is lately focused on the development of new membrane materials with increased performances like metal organic frameworks (MOFs), mixed matrix membranes (MMM) or composite carbon molecular sieve membranes (CMSM). These membranes, especially CMSM, can largely surpass the upper bound of polymeric membranes and are not affected by plasticization. In fact, the hydrocarbons contributing to this effect have been removed during the carbonization step and converted in a rigid carbon structure not affected by plasticization. However, the experience with these membranes is limited and still more research on the preparation methods and precursor materials are required, and economics evaluations are missing.

In this work a composite alumina-CMSM (Al-CMSM) is investigated for the selective separation of CO_2 from typical biogas compositions at different operating temperatures and pressures, and at different membrane activation temperatures. In view of the reduction in carbon emissions, in this work also the CO_2 separation from N_2 was investigated using typical gas compositions coming out of flue gases from industrial furnaces like in steam methane reforming or cracking units. The carbon membrane is supported on an alumina tube, which provides a much higher mechanical stability compared to hollow fibers modules, although at the expenses of a reduced surface area. These membranes have been prepared by the carbonization of a novolac polymeric precursor under an inert atmosphere, and their properties (pore size distribution or thermal resistance) can be fine-tuned by adjusting the carbonization temperature, inert gas atmosphere and pre- or post-treatments.

This work has also been extended with a detailed techno-economic analysis for H_2 production using Aspen Plus. In particular, this analysis compares the thermodynamics and the costs of H_2 production using the conventional technology powered with natural gas or with upgraded biogas. This is important in view of the expected revamping of existing plants in the coming future when biofuels take over the fuel processing market.

In the coming section first the membrane preparation, experimental setup and experimental conditions investigated are described. Subsequently, the methodology and the plant layouts of the different configurations investigated for the techno-economic analysis are given. Finally, the experimental results are presented and are afterwards used for the design of biogas upgrading systems to be implemented in conventional H_2 production plants, and their impact on the economics is described.

2. Experimental methods

2.1. Membrane preparation

A detailed description of the preparation method of the novolac phenolic resin precursor material and the membrane itself can be found in a previous work reported in the literature [17]. In general, the membrane preparation method consists of three consecutive steps: 1) dip coating of the porous support, 2) drying and 3) carbonization in inert atmosphere.

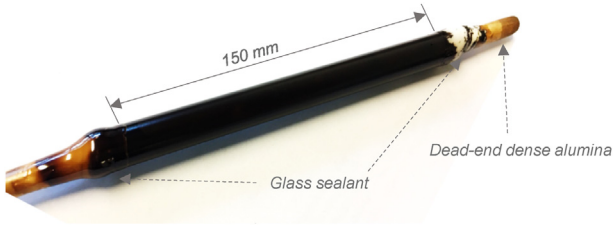

Fig. 1. Image of the resulting composite carbon molecular sieve membrane.

Before the impregnation of the carbon-based precursor, the porous alumina tube (α-Al_2O_3 with 200 nm pore size) is fixed to dense alumina tubes using glass sealants, resulting in a dead-end configuration. This means that one of the sides is properly closed, while the other one remains open. The resulting porous tube is 150 mm in length, and 10/7 mm outer/inner diameter. The alumina tube is immersed for 10 s in N-Methyl-2-pyrrolidone solution containing 13% of novolac solution, 0.8% of nanoparticles of bohemite (Kawaken Fine Chemicals Co., Ltd.), 2.4% of formaldehyde and 0.6% of ethylene-diamine (all in %wt.). Afterward, the coated tube is dried overnight at 100 °C under continuous rotation inside an oven. Finally, the membrane is carbonized in N_2 atmosphere (200 ml/min) at 500 °C for 2 h using a heating rate of 1 °C/min. An image of the resulting composite carbon membrane is depicted in Fig. 1.

2.2. Experimental

The open side of the dense tube was connected to 6 mm stainless steel tube using graphite ferrules and standard Swagelok components. The Al-CMSM membrane was assemble into a stainless-steel reactor located inside an electrical oven. The feed gases were controlled by mass flow controllers (Bronkhorst B.V.) and downstream the reactor, a back-pressure controller regulates the system pressure. The permeate side of the membrane was connected to a diaphragm vacuum pump (VWR PM20404-820.3) to maximize the difference in partial pressure at both sides of the membrane. The outlet of the vacuum pump is at atmospheric conditions and it was sent either to a μ-GC (Varian CP-4900) to measure the permeate compositions, or to a film-flow meter (Horiba Stec VP3) to determine the permeation fluxes through the membrane. A detailed process flow diagram of the experimental setup used in this work is represented in Fig. 2.

The Al-CMS membranes show hydrophilic behavior, and when exposed to ambient conditions tend to adsorb humidity, partly blocking the pores [17]. Therefore, an important task of the experimental screening was to activate the membrane by removing the water adsorbed in the pores. In this process, water removal leads to a modification in the permeation properties of the membranes and thus, its investigation is also of interest. This was done by increasing the temperature in an inert gas (helium) at pressurized conditions (4 bar (a)) and, in this work, the activation temperature was varied from 100 to 200 °C. For the two different gas mixtures investigated in this work, CO_2/N_2 and CO_2/CH_4, different compositions, pressures and permeation temperatures were selected. An overview of the experiments carried out in this work is presented in Table 1.

3. Techno-economics

3.1. Description of the process schemes

The process schemes and the methodology used for the techno-economics were adopted from the work of Spallina et al. [18], who compared the costs of H_2 production with novel technologies based on membrane reactors, with the established benchmark steam methane reforming process, with and without carbon capture. In this work, first a conventional H_2 production scheme (*Case 1*) was designed and

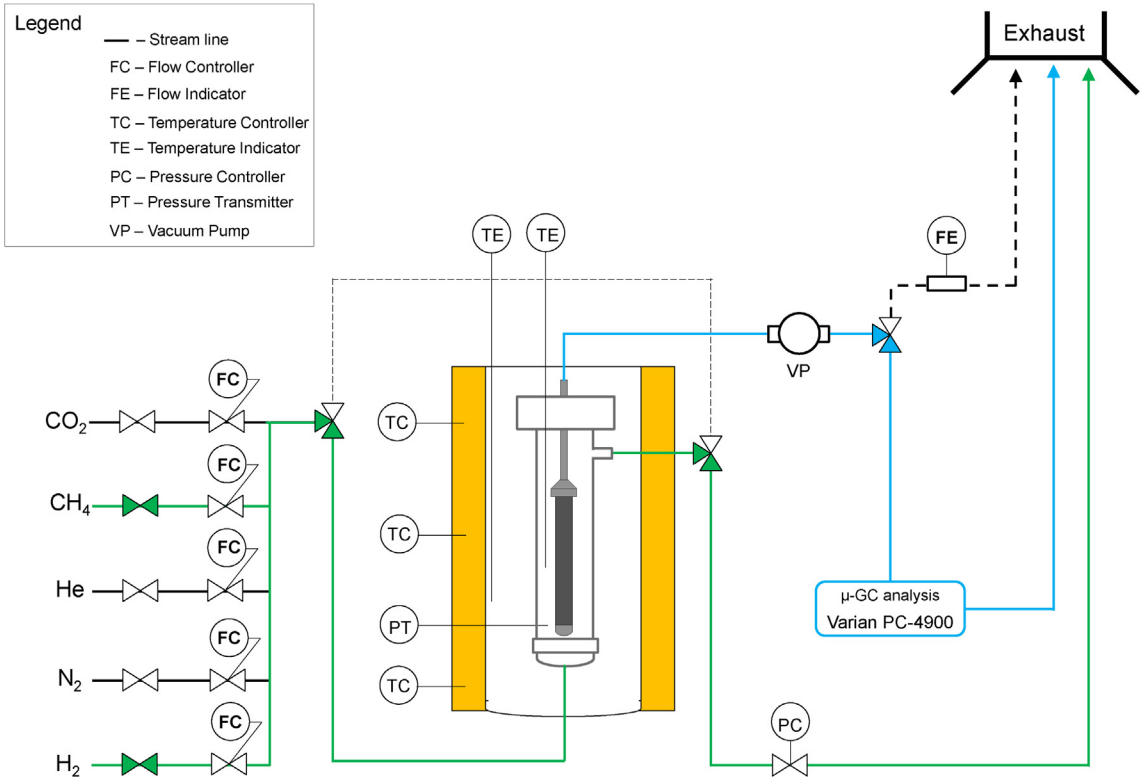

Fig. 2. Process flow diagram of the experimental setup used in this work.

Table 1
List of experiments carried out in this work.

Parameters	CO_2/CH_4 mixture	CO_2/N_2 mixture
Activation temperatures [°C]	100, 150 and 200	100-150-200
Permeation temperature [°C]	30, 40, 60, and 80	30, 40, 60, and 80
Operating pressure [bar(a)]	3–7	3–7
Gas composition (CO_2/X) [%vol.]	80/20; 60/40; 45/55; 30/70; 10/90	10/90; 20/80; 30/70

validated with results from the literature [18] and, subsequently, three more configurations are investigated.

The first modified process scheme uses the results obtained for CO_2/N_2 separation mixtures. In this case, natural gas is used as feedstock material, and the CO_2 is captured using CMSC membrane modules installed in the flue gas stream at the outlet of the convective section of the burner of the reforming reactor (*Case 2*). Another alternatives and also in view of the revamping of currently installed H_2 production plants, use biogas as feedstock for H_2 production. In a first case, biogas is directly fed into the system and all the CO_2 produced is released to the atmosphere since it does not come from anthropogenic sources (*case 3*). The last case investigated in this work uses the experimental data obtained with CMSC membranes and consists in upstream biogas upgrading in order to increase the energy density of the fuel used for H_2 production (*case 4*). In this case, the CO_2 permeated through the membranes is emitted to the atmosphere. The general process scheme and the different alternatives investigated in this work are presented in Fig. 3.

In this scheme, natural gas from the grid or (updated) biogas is fed into the process and is mixed with steam to achieve the correct steam to carbon (S/C) ratio to avoid carbon formation. Before that, the sulfur contained in the natural gas is removed over a ZnO bed in the desulphurization stage. When biogas is used as feedstock, it is assumed to be clean. The gas mixture is then fed into a pre-reformer reactor operated at 490 °C. The pre-reformed gas mixture is subsequently fed into a top fired tubular reformer operated at 890 °C and 32.7 bar where the syngas is produced through reaction (1). The reformer reactor consists of multiple small and long tubes filled with a Ni-based catalysts. The syngas is sent to a high-temperature WGS reactor passing first through syngas coolers where high pressure steam is produced. The WGS reactor operates at temperatures between 330 and 430 °C and is filled with Fe-Cr catalysts, and the man reaction occurring is given in reaction (2). In this case a single WGS unit is selected, omitting the common low temperature WGS, since the unconverted CO is downstream sent to the burner, which overall allows a better heat integration. The H_2-rich outlet gas of the WGS unit is cooled down in order to condense all the steam and is subsequently sent to a PSA unit with a recovery efficiency of 89% for a H_2 purity of 99.999%. The PSA off gas is mixed with make-up fuel and is combusted inside the reformer module to provide the heat required by the highly endothermic reforming reaction. The burner temperature is normally above 1000 °C and is first used for steam production and subsequently for heat integration by heating up the feed gases. The gas stack is a gas mixture containing mainly N_2, CO_2, steam and excess O_2 and is normally emitted at 150 °C.

$$\textit{Steam Methane Reforming} \quad CH_4 + H_2O \leftrightarrow CO + 3H_2 \tag{R1}$$

$$\textit{Water GasShift} \quad CO + H_2O \leftrightarrow CO_2 + H_2 \tag{R1}$$

Only when natural gas is used as fuel source, the CO_2 emitted to the atmosphere contributes to the climate change. Therefore, a post-combustion membrane unit was installed in one of the selected strategies (*case 2*). In this case, the gas stack is first cooled down to condense all the steam and it is subsequently compressed to 30 bar. The gas mixture passes through a first stage membrane module where CO_2 is recovered until a pressure gradient between the feed side and the permeate side is 0.5 bar. Since the purity of the CO_2-rich permeate gas does not achieve the requirements for carbon capture [2], a second membrane stage is used. This means that an inter-stage compressor is required, and it pressurizes the gas again to 30 bar. In both membrane modules, the retentate gas is emitted to the atmosphere, and the small amount of CO_2

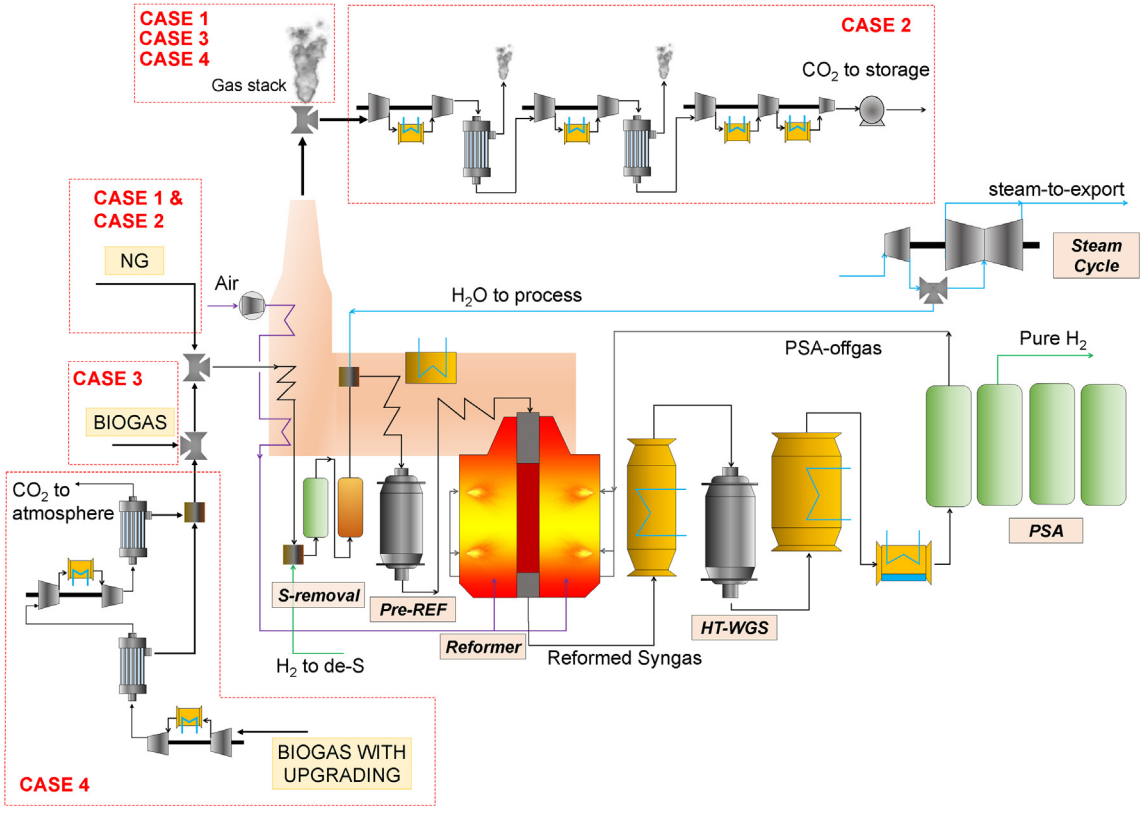

Fig. 3. Process scheme of the different strategies selected. Case 1 uses natural gas as feedstock and CO_2 is not captured; Case 2 uses natural gas as feedstock and the CO_2 is captured using CMSC membranes; Case 3 uses biogas as feedstock; Case 4 uses bio-methane produced from the upgrading of biogas using CMSC membranes.

contained on it represents the net CO_2 emissions of this technology.

Similarly as in post-combustion, the biogas is upgraded in one of the selected process schemes (case 4). The upgrading is carried out by means of a two-stage membrane module with an inter-stage compressor to avoid methane losses. In this case, the upgraded biogas remains at high pressures, while the CO_2 separated is emitted to the atmosphere. If this CO_2 is to be conditioned for capture, this process will lead to an overall negative carbon emissions which is also foreseen as potential strategies to reduce the CO_2 concentration in Earth, although this possibility has not been investigated in this work. In this strategy, the biogas is first compressed to 35 bar, and the permeate gas, a gas mixture rich in CO_2 is again compressed to 35 bar to minimize the methane losses. The retentate from both membrane modules, which are streams rich in CH_4, are mixed and sent directly into the process, resulting in a gas stream with a methane purity of 89%, and methane losses below 0.1%.

3.2. Methodology and assumptions

The methodology used in this work is also similar to the one adopted by Spallina et al. [18], who also investigated the cost of hydrogen in a conventional H_2 production plant. The main assumptions of the turbomachinery and operating conditions used in this work for the different plant configurations are provided in Table 2. Also, since the CMSC membranes are used in this work as a technology to reduce the carbon footprint, different parameters involving reforming efficiencies, fuel consumptions and CO_2 emissions are evaluated. In particular, in Eqs. 1–7 the different parameters for a thermodynamic analysis are provided.

Equivalent natural gas flow rate

$$\dot{m}_{NG,eq} = \dot{m}_{NG} - \frac{Q_{th}}{\eta_{th,ref} \bullet LHV_{NG}} - \frac{Wel}{\eta_{el,ref} \bullet LHV_{NG}},$$

$$\text{With} \quad \eta_{th,ref} = 0.9 \text{and} \eta_{el,ref} = 0.583 \tag{1}$$

Steam export

$$Q_{th} = \dot{m}_{NG} \bullet (h_{steam@6bar} - h_{liqsar@6bar}) \tag{2}$$

H_2 production efficiency

$$\eta_{H_2} = \frac{\dot{m}_{H_2} \bullet LHV_{H_2}}{\dot{m}_{NG} \bullet LHV_{NG}} \tag{3}$$

Equivalent H_2 production efficiency

$$\eta_{H_2,eq} = \frac{\dot{m}_{H_2} \bullet LHV_{H_2}}{\dot{m}_{NG,eq} \bullet LHV_{NG}} \tag{4}$$

CO_2 specific emissions (E_{CO2})

$$E_{CO_2} = \frac{\dot{m}_{CO_2,capt}}{\dot{m}_{NG} \bullet LHV_{NG} \bullet E_{NG}} \tag{5}$$

Equivalent CO_2 specific emissions ($E_{CO2,eq}$)

$$E_{CO_2,eq} = \frac{\dot{m}_{CO_2,capt} - Q_{th} \bullet E_{th,ref} - W_{el} \bullet E_{el,ref}}{\dot{m}_{NG} \bullet LHV_{NG} \bullet E_{NG}},$$

$$with \quad E_{th,ref} = 63.3 \frac{g_{CO2}}{MJ_{th}} \quad \text{and} \quad Eel, ref = 97.7 \frac{g_{CO2}}{MJ_{el}} \tag{6}$$

Equivalent specific primary energy consumption for CO_2 avoided ($SPECCA_{eq}$)

$$SPECCA_{eq} = \frac{\frac{1}{\eta_{H_2,eq}} - \frac{1}{\eta_{H_2,eq,ref}}}{E_{CO_2,ref} - E_{CO_2,eq,ref}} \bullet 1000 \left[\frac{MJ_{th}}{kg_{CO_2}} \right] \tag{7}$$

Table 2
List of working conditions and assumptions for the thermodynamic analysis.

Case number	1	2	3	4
Fuel gas	Natural gas	Natural gas	Biogas	Biogas
Upgrading	–	–	–	CMSC membrane
CO_2 capture	–	CMSC membrane	–	–
Fuel composition	89% CH_4; 7% C_2H_6; 1% C_3H_8; 0.11% C_4H_{10}; 2% CO_2; 0.89% N_2		67% CH_4; 30% CO_2; 3% N_2	
Operating conditions for all the cases				
Steam to carbon: 2.7				
Furnace temperature: 1010 °C				
Pressure drops in the reactors: 1% (inlet pressure)				
Pre-reforming: 550 °C				
Reforming reactor temperature: 890 °C				
Reforming reactor pressure: 32.7 bar				
Water gas shift reactor inlet temperature: 340 °C				
PSA H_2 separation purity: 89%				
PSA H_2 separation pressure: 29.7 bar				
Compressors H_2 delivery				
Heat exchangers				
ΔT_{min} gas–gas: 20 °C				
ΔT_{min} gas–liquid: 10 °C				
Pressure drops: 2% (inlet pressure)				
U gas–gas: 35 W m^{-2} K^{-1}				
U gas–water: 50 W m^{-2} K^{-1}				
Number of stages: 3				
H_2 delivery conditions: 30 °C and 150 bar				
Compressors CMSC membranes modules and compressor for CO_2 storage				
Number of stages CO_2/N_2 compressors: 2				
Discharge pressure and temperature: 30 bar and 40 °C				
Number of stages CO_2 compressor				
Delivery conditions CO_2: 110 bar and 30 °C				
Number of stages biogas upgrading compressors: 2				
Discharge pressure and temperature: 35 bar and 40 °C				
Steam cycle				
Inlet steam conditions: 485 °C and 92 bar				
Isentropic efficiency first stage steam turbine: 75%				
Discharge pressure first stage: 34 bar				
Isentropic efficiency second stage steam turbine: 75%				
Steam export con				
ditions: 6 bar				

3.3. Economic analysis

The approach adopted for the economic analysis is based on the methodology used by the National Energy Technology Laboratory (NETL) [19]. The cost assessment is done by the comparison of the cost of hydrogen (COH), defined by the CCS institute [20] as presented in Eq. (8).

$$COH = \frac{(TOC \bullet CCF) + C_{O\&M,fix} + (C_{O\&M,var} \bullet h_{eq})}{\dot{N}_{H_2} \bullet 22414 \bullet 3600 \bullet h_{eq}} \quad (8)$$

In this case the total overnight costs (TOC) are function of the total capital expenses, and are calculated as in Table 3. The TOC is used to calculate the COH by using the capital charge rate factor (CCF), which is characteristic unit cost of the plant over the life time and a value of 0.153 applies as suggested in the literature. For the cost of each component, data was taken from the literature, and an overview of these costs is depicted in Table 4.

In Eq. (8) the operating and maintenance costs (O&M) are also included, which are divided in two different parts. On the one hand, the fixed costs, which account for the insurances and replacements. On the other hand, the variable costs include the costs of fuel, electricity, water, etc. A summary of the main assumptions selected for the calculation of the O&M costs is presented in Table 5. Finally, the h_{eq} refers to the equivalent working hours of the plant, and in this case it is assumed an availability of 90%.

These data are used to scale the costs to the actual capacity with the formula

$$C_i = C_0 \bullet \left(\frac{S_i}{S_0}\right)^n$$

4. Results

4.1. Experimental results

Single gas permeation measurements have been carried out in order to determine the ideal perm-selectivity of the Al-CMS membrane for the separation of CO_2 from N_2 and CH_4. These measurements have been carried out after membrane activation at different temperatures, particularly at 100 and 150 °C, and the gas permeation was measured at different temperatures ranging from 30 to 80 °C. As it can be seen in Fig. 4, for an activation temperature of 150 °C, the permeance of the gases follows a trend based on the kinetic diameter, except for helium, which shows lower permeances compared to H_2. This behavior was previously reported in the literature and is associated to a larger adsorption affinity of H_2 in carbon membranes compared to He, and also to the smaller cross-section diameter of H_2, which shows less resistance to gas transport through the pores by molecular sieving mechanisms [26]. A similar effect is also observed with CO_2, which is adsorbed by the porous of the carbon membrane. Therefore, the gas permeation measured is a combination of molecular sieving and adsorption diffusion mechanisms.

From single gas permeation results at various operating temperatures and activation temperatures, the activation energies (E_a) have been calculated using the Arrhenius plot of the permeance (J) with the inverse of the temperature (T) (Eq. (9)), being R the ideal gas constant.

$$J_i = \frac{P_0}{t} \bullet \exp\left(-\frac{Ea}{RT}\right) \bullet \Delta P_i \Rightarrow LnJ = \frac{Ea}{R}\left(\frac{1}{T}\right) + c \quad (9)$$

The apparent activation energy E_a is a contribution of molecular sieve and adsorption diffusion mechanisms. Gases with high kinetic diameters will show higher resistances to pass through the pores when decreasing the temperature, and this effect is more remarkable for gases with a diameter in the same range of the mean pore size diameter of the CMSC membrane. In addition, the adsorption of gases by the bigger micropores decreases with the temperature. A summary of these results is presented in Table 6, and some conclusions can be discussed.

First, it is verified that by activating the membrane at higher temperatures, the activation energy is decreased. This is observed for every gas and it is explained by the fact that the pores of the membrane become larger as consequence of the higher removal of adsorbed water in the pores, thus facilitating the permeation of gases. Also, it is concluded that the activation energy increases as function of the kinetic diameter as consequence of the molecular sieving mechanism. Furthermore, for

Table 3
TOC calculation methodology [19].

Plant component	Cost (M€)
Component W	A
Component W	B
Component W	C
Component W	D
Bare Erected Cost (BEC)	A + B + C + D
Direct costs as percentage of BEC instrumentation, civil work, etc.	
Total installation costs [TIC]	80% BEC
Total Direct Plant Costs [TDPC]	BEC + TIC
Indirect costs [IC]	14% TDPC
Engineering procurement and construction [EPC]	TDCP + IC
Contingencies and owner's costs (C&OC)	
Contingency	15% EPC
Owner's cost	10% EPC
Total contingencies and owner's costs [C&OC]	15% EPC
Total Overnight Costs [TOC]	EPC + C&OC

Table 4
List of assumptions for the costs of each component for reference capacities*.

Equipment	Scaling Parameter	Ref. Capacity, S_0	Ref. cost, C_o (M€)	Scale factor, f	Cost year	Ref.
Desulphurizer	Thermal plant input [MW_{LHV}]	413.8	0.66	0.67	2011	[21]
WGS Reactors		1246.06	9.54	0.67	2007	[22]
Reformer		1246.06	42.51	0.75	2007	[22]
Pre-reformer		1800	17.50	0.75	2005	[23]
PSA Unit	Inlet flow rate [kmol/h]	17,069	27.96	0.6	2007	[22]
H_2 Compressor	Power [HP]	1	0.0012	0.82	1987	[24]
Blower	Power [MWel]	1	0.23	0.67	2006	[23]
Steam Turbine	ST gross power [MWel]	200	33.70	0.67	2007	[21]
Cooling systems	Heat rejected [MW]	13.19	17.18	0.67	2007	[22]
CMSC membranes	Area [m^2]	1	1000	0.67	2016	[25]
Biogas compressor	Power [MWel]	13	9.9	0.67	2009	[21]
CO_2 compressor	Power [MWel]	13	9.9	0.67	2009	[21]
Heat exchangers	Area [m^2]	1	2000	0.67	2016	[18]
Economizers	Heat duty [kW]	1	86	0.67	2016	[18]

Table 5
Assumptions for the calculations of the O&M costs [18].

O&M fixed		
Labor costs	M€	1.5
Maintenance costs	%TOC	2.5
Insurance	%TOC	2.0
O&M variable		
Catalyst and sorbent replacement	$/kg	15
Reforming catalyst cost	k€/m^3	50
Water gas shift catalyst cost	k€/m^3	14
Desulphurization catalyst cost	$/$ft^3$	355
Lifetime	years	5
Consumables		
Cooling water make-up cost	€/m^3	0.35
Water cost	€/m^3	2
Natural gas cost	€/GJ_{LHV}	9.15
Biogas cost	€/GJ_{LHV}	9.15(1)
Steam cost	€/ton	0.13
Electricity cost	€/MW_h	76.36

(1) Considering in the costs the biogas cleaning up.

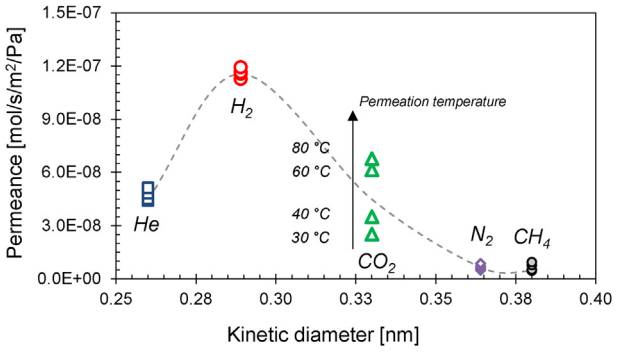

Fig. 4. Permeance of different gases as function of the kinetic diameter for the CMSC membrane activated at 150 °C.

Table 6
Activation energies measured for different gases at different activation temperatures.

Activation temperature [°C]	Activation Energy [kJ/mol] (kinetic diameter [nm])				
	He (0.26)	H_2 (0.29)	CO_2 (0.33)	N_2 (0.36)	CH_4 (0.39)
100	2.89	5.59	24.7	28.7	46.6
150	2.85	0.97	17.2	8.4	12.7

those gases with high adsorption affinity, like CO_2, the activation energy measured is higher than the one expected just based on the kinetic diameter as a consequence of the combined adsorption-diffusion effect of these carbon-based gases. The values of activation energy found indicate that in case the membrane is activated at 100 °C, the mean pore size of the membrane is in the range of 0.36–0.39 nm since the activation energy experiences an important increase in that range. On the other hand, when activating the membrane at 150 °C, the mean pore size is shifted towards bigger pores, and the mean pore size is larger than 0.39.

Afterward, gas permeation was evaluated for biogas and burner off-gas synthetic mixtures. The adsorption of CO_2 in the pores of the membrane will lead to the blockage of these pores, thus limiting other gases to pass through the membrane. This is expected since CO_2 shows the highest adsorption affinity compared to N_2 and CH_4, and overall it has the capacity to fine tune the CO_2 selectivity. The results are presented for different gas compositions, activation temperatures and permeation temperatures, and these results have been incorporated in a revised Robeson plot with the upper bound of polymeric membranes.

Fig. 5 (left) presents the results of CO_2 permeation and the purity in the permeate side for post-combustion gas mixtures (CO_2/N_2). The results are presented as a function of the gas feed composition and for several permeation temperatures after activation at different temperatures. Compared to permeation measurements for single gases (Fig. 4), the permeability of CO_2 remains constant for measurements carried out at the same operating temperatures and activation temperatures. For example, the CO_2 permeance measured at 40 °C after an activation temperature of 150 °C is 3.48 × 10^{-8} mol/s/m^2/Pa and, in the case of a gas mixture containing 10% CO_2 (vol.), the CO_2 permeance is 3.55 × 10^{-8} mol/s/m^2/Pa. Similar results are measured for other operating conditions. On the other hand, based on ideal perm-selectivity measurements, the CO_2 purity expected in the permeate at that operating conditions should be around 40%. However from gas mixture measurements the measured CO_2 purity from gas chromatography analysis is 75%. This indicates that CO_2 is indeed limiting the permeation of N_2 through the membrane as a consequence of CO_2 adsorption in the pores.

It is also observed that the CO_2 concentration in the feed has a major effect on the separation through the membrane. In particular, when the feed is more diluted in N_2 lower CO_2 purities are obtained from the membrane, and thus another membrane stage would be required to obtain CO_2 concentrations suitable for capture. On the other hand, the activation temperature, compared to the operating temperature, seems to have a minor impact on the separation properties. This is explained by the fact that CO_2 is highly adsorbed on the carbon surface at the operating temperatures used experimentally. At the steady state, the water that was removed will be replaced by CO_2 and will create an effect of pore blocking. This effect depends on the operating

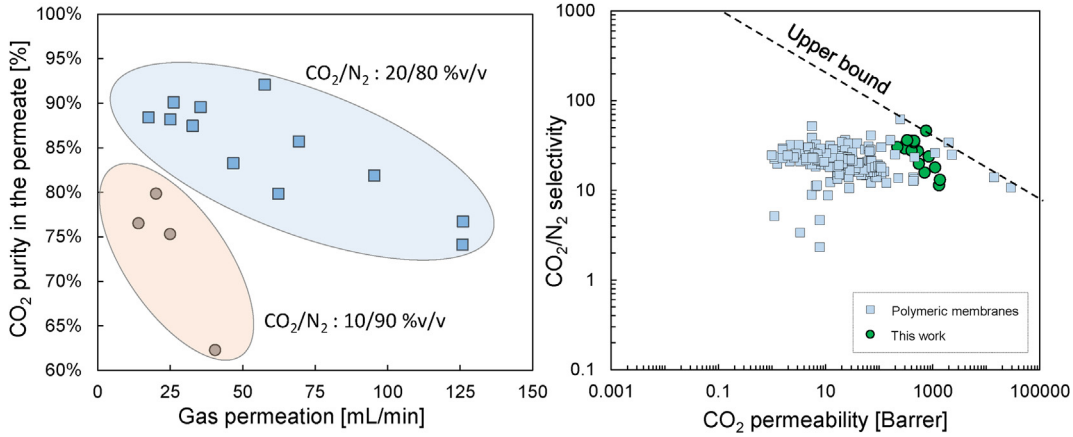

Fig. 5. Left: Gas permeation results for CO_2/N_2 mixtures at different operating conditions and right: Robeson plot for CO_2/N_2 separation.

temperature and, in the case of CO_2, the higher the temperature the lower the extent of adsorption [27]. Therefore, the two compositions investigated follow a linear decreasing trend with a compromise between purity and permeation. The values giving the lowest purities of CO_2 and highest permeations have been obtained at high temperatures (80 °C), while the values of high purities and low permeations are obtained at low temperatures (30 °C). For all these measurements, the feed pressure was 7.5 bar(a), while the permeate was kept at vacuum conditions.

On the other hand, in Fig. 5 (right) the Robeson plot of this gas mixture system is given with data of polymeric membranes from literature and the results obtained experimentally for the CMSM membrane investigated in this work. From the results, it is observed that the CMSM is located at the upper bound of the polymeric membranes, with the main advantage that stability is not compromised.

Similar experiments have also been carried out for biogas upgrading mixtures. Fig. 6 (left) shows the gas permeation and the CO_2 purity for two gas mixtures containing 45 and 30% of CO_2 in CH_4. The results presented are from experiments carried out at different permeation temperatures (up to 80 °C) and membrane activation temperatures (up to 200 °C).

The general conclusions that can be obtained for this gas mixture are similar to the ones given for CO_2/N_2 mixtures. In this case, both gases are adsorbed on the carbon surface, and thus there is a competition between them. This has implied, in average, a decrease of about 40% in CO_2 permeability through the membrane as compared with single gas permeation tests. On the other hand, the selectivity measured for this gas mixture has experienced a slight increase (6% in average) for all the operating conditions investigated compared to ideal perm-selectivity values obtained from single gas experiments. This also indicates that CO_2 has a stronger adsorption on the carbon surface compared to CH_4 at the same temperature, as also previously indicated in the literature [27].

In this gas mixture, the operating temperature has a major effect on the membrane performance. Similar as in CO_2/N_2 mixtures, a decreasing trend in selectivity-permeability is observed when increasing the operating temperature. In particular, higher selectivities are obtained when working at low temperatures, which was also expected from ideal perm selectivity measurements. In this case, CO_2 permeation presents higher surface diffusion mechanisms over CH_4 at low temperatures, and thus these higher selectivities can be expected. This leads to results that are located at the upper Robeson bound (Fig. 6 right) and, for some specific operating conditions (mostly at low operating temperatures), the permeation characteristics are located slightly above this empirical threshold found in polymeric membranes.

In the CO_2/N_2 post-combustion mixtures, where only CO_2 is adsorbed in the pores and the kinetic diameter of both gases is very similar, the CMSC membrane has shown an increase in its performance in the case of a gas mixture. However, for biogas mixtures, the competition of the two main components leads to a decrease in the CMSC membrane performance, even if there is a larger difference in the kinetic diameter of the two gases. In order to improve the performance of the membrane, a modification in the carbonization temperature/atmosphere could limit the mean pore size, and more research is required in this field.

Still the CMSC membrane shows an improved performance compared to the upper bound of polymeric membranes and with the potential to overcome the drawbacks of plasticization in presence of CO_2.

The results presented in this section are subsequently used in the techno-economic analysis for the design of a membrane separation

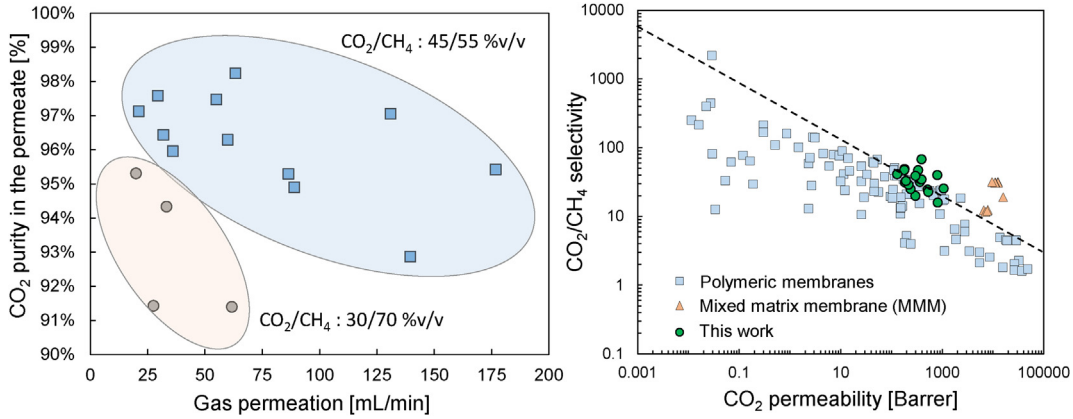

Fig. 6. Left: Gas permeation results for CO_2/CH_4 mixtures at different operating conditions and right: Robeson plot for CO_2/CH_4 separation.

module for CO_2 capture and biogas upgrading, and the implication in the economics of the process.

4.2. Techno-economic comparison

Firstly the process scheme selected was validated with data presented by Spallina et al. [18]. The same operating conditions have been selected and the costs of each equipment have been calculated based on the assumptions and the methodology described in Section 3. A summary of the validation is given in Table 7.

The results obtained with the process scheme developed in this work are in good agreement with previously reported data in the literature. The small deviations observed in the electricity and economics can be associated to slightly different operating conditions for the heat integration in the convective section as well as in the syngas coolers. These results also lead to a small deviation in the efficiencies and in the cost of hydrogen to a maximum of 3%. The highest deviation observed from Table 7 corresponds to the net electric power. In the reference case, the net power is almost 0, which means that a small net deviation results in a large relative deviation. This happens because the net electric power is a sum of electricity consumptions from pumps and compressors, and productions from the steam turbine. In fact, the average deviation of each individual component is just 4.5%, mostly associated to deviations in the H_2 compressor and the steam turbine. These deviations are associated to the slightly lower H_2 production and possible differences in the assumptions of the steam turbine. Once the main process scheme is validated with data from the literature, the different modifications integrating membrane modules have been implemented.

In the case of post-combustion carbon capture (case 2), a membrane module is designed at the exhaust gas from the convective section of the burner. This stream is at atmospheric pressure and, after the heat recovery, first the steam is condensed in order to remove humidity that can modify the performance of the membrane. The dry stream is subsequently compressed to 30 bar and the gas is sent to a first stage membrane module at 40 °C. The dry gas has a composition of around 20% CO_2 (vol.), and thus its design is carried out based on the experimental results obtained for the mixed gas experiments presented in the previous section. In this stage it is assumed a CO_2 separation until the driving force (partial pressure of CO_2 at both sides of the membrane module) is 0.2 bar. The CO_2 purity at the permeate of this stage is 89%, which is in agreement with experimental results of the gas mixtures. Since the purity is not high enough for carbon capture, a second stage membrane module is needed. The permeate, which is at atmospheric pressure, is again compressed to 30 bar for further CO_2 purification. In this membrane module the purity of the CO_2 in the permeate is 99.8%, thus suitable for capture. Overall, it leads to a CO_2 recovery of 83.7%. The fraction of gas that has not permeated through the membrane, together with the one in the first module, is released to the atmosphere. The membrane area required in both stages is calculated based on the amount of gas permeated and the permeance measured experimentally.

In the biogas upgrading case, clean biogas is first compressed to 40 bar and it enters to a first membrane module, where the CO_2 permeates and the CH_4 concentrates in the feed side. In this first module, the CO_2 permeates until a partial pressure difference between the feed and permeate sides of 1.5, resulting in a stream with a CO_2 purity of 87.7%. In this first module, part of the methane (around 5%) permeates through the membranes and, in order to decrease the methane loses, a second stage membrane module is required. For this second stage, the permeate gas is first compressed to 40 bar and it enters the second membrane module. In this module, since the inlet is highly concentrated in CO_2, the permeate stream has a CO_2 purity of 99.8%, which could be conditioned for sequestration. The retentate gas is subsequently mixed with the retentate of the first module, and this gas mixture (87.6% in CH_4) is then fed in the process.

Subsequently, the four different cases have been compared from a thermodynamic point of view. For all of them, the operating conditions selected are similar, resulting in a fair comparison between the different cases. The results of this comparison are presented in Table 8, and several conclusions can be obtained:

- The thermal input selected for the four different cases is very similar, leading to similar H_2 production efficiencies. In order to achieve this similar thermal input, the feed flow rate of biogas should be 2.2 times higher compared to the natural gas feed flow rate.
- The conventional technology is the only one with a net electricity production in comparison to the other cases. The fact that the CO_2 is emitted to the atmosphere implies that expensive turbomachinery is not required, meaning that all the electricity generated by the steam turbine is able to power the whole plant. When the CO_2 is to be sequestrated, the installation of membrane modules at the exhaust of the burner leads to increased electricity consumptions. In particular, the N_2/CO_2 compressors are very expensive in terms of power consumption, and overall it leads to the need of electricity import.
- In the case biogas is used as feedstock material (cases 3 and 4), the main power consumption comes from the biogas compression to the process pressure. In particular, the first compression stage consumes already most of the electricity that can be generated by the steam turbine. In case 4, which includes the upgrading of the biogas, the power for the compression of the gas fed into the second membrane module slightly increases the total energy consumption of the process.
- Although the thermal input is similar for all the cases, some differences can be observed concerning the H_2 production efficiency. For the cases 1 and 2, exactly the same efficiency is obtained, since the only difference comes from the treatment of the exhaust gas stream in case 2. In case 3, the biogas fed into the reactors has 30% (vol.) of CO_2 in the feed. This leads to a decrease in the thermodynamic equilibrium, with a concomitant decrease in the reforming efficiency (0.70 compared to 0.72 of cases 1 and 2). On the other hand, in case 4 part of the CO_2 is removed in membrane modules, leading to an upgraded biogas feed containing less amount of CO_2. This results in reforming efficiencies (0.71) higher than the ones obtained in case 3, although still lower compared to cases 1 and 2.

Table 7
Detailed validation of the process scheme developed in this work with literature data [18].

Parameter	units	Spallina et al. [18]	This work	Deviation [%]
Overall comparison				
Feed flow rate	[kg/s]	2.62	2.62	0
Steam-to-carbon ratio	[−]	2.7	2.7	0
H_2 mass flow rate	[kg/s]	0.75	0.73	2.6
Electricity production/consumption				
Air compressor/ extraction fan	[MWel]	−0.68	−0.67	1.5
H_2 compressor	[MWel]	−2.77	−2.12	6.6
Steam turbine	[MWel]	3.27	3.44	−5.4
Pumps	[MWel]	−0.21	−0.20	4.7
Other auxiliaries	[MWel]	−0.05	−0.05	0
Net electric power	[MWel]	0.07	0.40	−482
Efficiencies and CO_2 emissions				
H_2 production efficiency	[%]	0.74	0.72	2.7
Eq. NG input	[kg/s]	2.41	2.40	0.42
Eq. H_2 production efficiency	[%]	0.81	0.79	2.9
CO_2 specific emissions	[kg_{CO2}/Nm^3_{H2}]	0.82	0.85	−3.2
Eq. CO_2 specific emissions	[kg_{CO2}/Nm^3_{H2}]	0.76	0.77	−2.0

Table 8
Thermodynamic comparison of the four different cases investigated in this work.

CASE	1	2	3	4
CO_2 capture technology	NO	Membranes	NO	NO
Feed	NG	NG	Biogas	Upgraded biogas
Feed flow rate [kg/s]	2.62	2.62	5.75	5.73
Feed thermal input [MW LHV, NG]	121.94	121.94	124.76	124.15
LHV feed [MJ/kg]	46.54	46.54	21.68	21.68
S/C ratio	2.70	2.70	2.70	2.70
H_2 mass flow rate [kg/s]	0.73	0.73	0.73	0.73
Electricity production/ consumption				
Air compressor/Air-exh fan [MW el]	−0.67	−0.69	−0.74	−0.98
H_2 compressor [MW el]	−2.12	−2.12	−2.12	−2.12
CO_2/biogas compressor [MW el]	–	−17.64	−3.36	−4.38
Steam turbine [MW el]	3.45	3.67	3.42	3.61
Pumps [MW el]	−0.20	−0.17	−0.16	−0.16
Other auxiliaries [MW el]	−0.05	−0.05	−0.05	−0.05
Net electric power [MW el]	0.41	−17.00	−3.01	−4.09
Steam export (160 °C, 6 bar) [kg/s]	4.02	4.02	4.02	4.40
H_2 production efficiency	0.72	0.72	0.70	0.71
Q_{th} [MW]	8.39	8.39	8.39	9.18
Equivalent NG input [kg/s]	2.40	3.05	5.56	5.58
Eq. H_2 production efficiency	0.78	0.62	0.73	0.73
Heat rate [Gcal/kNm^{3}H$_2$]	3.30	3.81	3.48	3.47
m CO_2 total emitted [g/s]	6900	2793	10,202	10,259
m CO_2 emitted [g/s] from fossil	6940	1132	0	0
m CO_2 emitted [g/s] from renewable	0	0	9908	9859
m CO_2 captured [g/s]	0	5808	0	0
m CO_2 from fossil for power generation [g/s]	−40	1661	294	400
CO_2 specific emissions [kgCO_2/kNm^{3}H$_2$]	0.85	0.14	0.00	0.00
Eq. CO_2 spec. em. [kgCO_2/ kNm^{3}H$_2$]	0.78	0.28	0.04	0.05
SPECCA [Gcal/kgCO_2]	–	0.72	0.20	0.19
Equivalent CO_2 avoided	–	64.49%	95.39%	93.74%

- When the net electricity production/consumption and thermal power are considered, the equivalent reforming efficiencies can be measured. In particular, in case 1, the equivalent reforming efficiency increases to a value of 0.78 resulting from the net electricity production and the availability of thermal power (Q_{th}). On the other hand, the high energy consumptions of case 2 lead to a sharp decrease in the equivalent reforming efficiency to a value of 0.62. This equivalent efficiency is lower than the one obtained by Spallina et al. [18], where the CO_2 was captured after the water gas shift stage in an absorption unit using MDEA as sorbent (0.67) material.
- In cases 3 and 4, the net electricity consumption is compensated by the steam that can be exported. This is observed in the decrease in the equivalent feedstock input, which slightly increases the equivalent reforming efficiency up to values of 0.73. In this case, it can also be noticed that the lower power consumptions of case 3 lead to a slightly larger increase in the equivalent reforming efficiency compared to case 4.

Finally, the economics of the different cases have been evaluated, and the comparison is depicted in Table 9. Similarly, as done for the thermodynamic comparison, some conclusions can be discussed:

The capital expenses of the case 1 is the lowest one and stands for the benchmark technology. When CO_2 is to be separated from the flue gas of the burner (case 2), there is the need of compressors and membranes. In this case, the compressor costs are high compared to cases 3 and 4, associated to the high flowrates (mostly N_2) in the exhaust. Furthermore, since the CO2 content in the exhaust line is highly diluted in N_2, its partial pressure in the first membrane module is limited. Therefore, there is the need of larger surface areas.

When biogas is used as feedstock material, the capital expenses are increased compared to the benchmark technology. On one hand, there is the need of compression since the biogas is produced at atmospheric pressure. On the other hand, since in the biogas some amounts of inert gases are present, larger units are needed. Overall, it results in increased capital expenses. In the situation of biogas upgrading (case 4), there is also the need of membrane modules, leading to slightly higher costs compared to case 3.

The cost of the feedstock material is somehow similar for all the cases. In particular, the biogas has a lower energy content, meaning that higher inlet flow rates are needed. However, since the cost depends on the energy content, the resulting costs for all the cases is similar.

The biggest difference comes from the electricity costs. While in case 1, there is a negative cost of electricity (it is produced), it represents a real cost for all the other ones. In case 2, the high energy demand associated to the compressors for the CO_2 removal from the exhaust gas leads to a very high costs (> 10 M€). Regarding the biogas cases, the one with upgrading (case 4) has a higher cost compared to case 3 since a second compression stage for the biogas upgrading is required.

When computing the capital and operation expenses, the cost of hydrogen with the technologies using biogas as feedstock material is 0.25 €/Nm^3, which is around 15% more expensive compared to case 1. When implementing CO_2 capture technologies (case 2), the cost of hydrogen largely increases to a value of 0.31 €/Nm^3, higher compared with the case where a MDEA adsorption unit is used (0.28 €/Nm^3) [18].

Finally, the costs associated to the reduction of carbon emissions to the atmosphere by the different strategies was evaluated and compared with the case 1. The results follow a similar trend as for the economics. The cost in case 2 is much higher compared with the others. There are two reason behind this high cost. On the one hand, less CO_2 is avoided compared to cases 3 and 4, mostly associated to the need of electricity. On the other hand, the cost of hydrogen is also higher, and thus, it comes to a high cost associated to reductions in CO_2 emissions.

5. Conclusions

In this work a composite Alumina molecular sieve carbon membrane was prepared by a simple dip coating method and subsequently tested for the separation of CO_2 from N_2 and CH_4. The activation of the membrane (heat treatment) removes water adsorbed on the pores of the membrane increasing the pore size and consequently their permeation properties. These membranes can find application in post-combustion CO_2 capture, meaning the separation of the CO_2 from N_2 in the exhaust gases in burners, and also as for the upgrading of renewable sources like biogas. These two applications have been experimentally investigated in this work. From the experimental results, it was observed that these membranes show a gas separation based on two different mechanisms, molecular sieving and selective adsorption. Owing to this combined mechanism, CO_2 can be separated from N_2 and CH_4 selectively, and the results measured for these two gas mixtures are slightly above the empirical Robeson limit of polymeric membranes. Since these membranes do not suffer from plasticization in the presence of CO_2, they could find industrial application in the coming years for gas separation.

In view of the potential use of these membranes at industrial scale, a detailed techno-economic analysis was performed for four different configurations for H_2 production using natural gas and biogas as feedstocks. First the conventional technology was validated with data reported in the literature, and it is was observed that installing CMSC membrane modules at the exhaust of the burner to recover the CO_2 emitted by the process is a very expensive route in order to reduce carbon emissions. In fact, the compression costs (in terms of electricity

Table 9
Summary of the economics of the four different cases investigated in this work.

Economics *CASE number*	1		2		3		4	
BEC [M€] (%)	37.64		58.35		44.59		46.67	
Desulphurizer	0.29	(0.8%)	0.29	(0.5%)	–	–	–	–
WGS reactor	2.23	(5.9%)	2.23	(3.8%)	2.64	(5.9%)	2.51	(5.4%)
Reformer reactor	8.26	(22.0%)	8.26	(14.2%)	9.96	(22.3%)	9.32	(20.0%)
Pre-reformer reactor	2.90	(7.7%)	2.90	(5.0%)	3.98	(8.9%)	3.71	(7.9%)
PSA unit	8.46	(22.5%)	8.46	(14.5%)	9.12	(20.5%)	8.68	(18.6%)
H_2 compressor	1.47	(3.9%)	1.47	(2.5%)	1.47	(3.3%)	1.47	(3.2%)
Blower	0.21	(0.6%)	0.21	(0.4%)	0.22	(0.5%)	0.27	(0.6%)
Steam turbine	3.06	(8.1%)	3.18	(5.5%)	3.05	(6.8%)	3.16	(6.8%)
Cooling system	10.75	(28.6%)	10.60	(18.2%)	9.67	(21.7%)	10.18	(21.8%)
CO_2 compressor	–	–	18.18	(31.2%)	4.47	(10.0%)	6.44	(13.8%)
Membranes	–	–	2.55	(4.4%)	–	–	0.92	(2.0%)
TOC × CCF [M€]	13.59		21.07		16.10		16.85	
O&M fixed [M€]	5.98		8.18		7.33		7.53	
O&M variables [M€]								
Process water	0.60		0.60		0.62		0.62	
Natural gas	31.67		31.67		0.00		0.00	
Biogas	0.00		0.00		33.50		32.60	
Steam cost	−0.01		−0.01		−0.01		−0.02	
Electricity costs	−0.25		10.23		1.81		2.46	
Cost of H_2 [€/Nm^3]	0.222		0.308		0.255		0.258	
Cost of H_2 variable	0.137		0.182		0.154		0.153	
Cost of H_2 fixed	0.084		0.126		0.101		0.105	
Cost of CO_2 avoided [€/t_{CO2}]			121.93		39.30		42.82	
Cost of CO_2 eq. avoided [€/t_{CO2}]			172.41		44.90		49.78	

and capital investments) become the bottleneck for this case, and just 65% of the total emissions can be reduced, also with a corresponding increase of about 40% in the cost of hydrogen.

On the other hand, using biogas as feedstock appears as an interesting strategy for a reduction in carbon emissions and revamping of existing plants. It was observed that upgrading biogas with carbon membranes yields higher reforming efficiencies. However, the increased number of equipment (and electric consumptions) leads to equivalent efficiencies and costs of hydrogen similar as if upgrading of the biogas is not considered. Overall, both strategies lead to reductions in carbon emissions to about 95%, with a concomitant increase in the cost of hydrogen to about 15%.

In order to further promote carbon membranes, it is still important to better understand their separation mechanism and how the post-treatment of the membranes and operating conditions can fine-tune the permeation and selectivity towards the desired requirements. In particular, it was observed that more selective membranes are still required in order to remove the need of a second membrane module, which nowadays also represents a limitation for polymeric membranes.

Declaration of Competing Interest

The authors declare that they have no known competing financial interests or personal relationships that could have appeared to influence the work reported in this paper.

References

[1] IPCC, Climate Change 2014: Synthesis Report. Contribution of Working Groups I, II and III to the Fifth Assessment Report of the Intergovernmental Panel on Climate Change, 2014.
[2] IPCC, IPCC special report on carbon dioxide capture and storage, Cambridge University Press, Cambridge (UK), 2005.
[3] IEA, Energy technology perspectives: scenarios and strategies to 2050, Paris, France: OECD/IEA, 2010.
[4] P. Weiland, Biogas production: current state and perspectives, Appl. Microbiol. Biotechnol. 85 (2010) 849–860.
[5] J.I. Huertas, N. Giraldo, S. Izquierdo, Removal of H2S and CO2 from biogas by amine absorption, in: J. Markos (Ed.), Mass Transf. Chem. Eng. Process., 2011: p. 318.
[6] E. Ryckebosch, M. Drouillon, H. Vervaeren, Techniques for transformation of biogas to biomethane, Biomass Bioenergy 35 (2011) 1633–1645.
[7] H.F. Abbas, W.M.A. Wan Daud, Hydrogen production by methane decomposition: a review, Int. J. Hydrogen Energy 35 (2010) 1160–1190.
[8] M. Valdés, M.D. Durán, A. Rovira, Thermoeconomic optimization of combined cycle gas turbine power plants using genetic algorithms, Appl. Therm. Eng. 23 (2003) 2169–2182.
[9] S. Das, J. Ashok, Z. Bian, N. Dewangan, M.H. Wai, Y. Du, A. Borgna, K. Hidajat, S. Kawi, Silica-Ceria sandwiched Ni core–shell catalyst for low temperature dry reforming of biogas: coke resistance and mechanistic insights, Appl. Catal. B Environ. 230 (2018) 220–236.
[10] D. Pakhare, J. Spivey, A review of dry (CO 2) reforming of methane over noble metal catalysts, Chem. Soc. Rev. 43 (2014) 7813–7837.
[11] S.D. Angeli, G. Monteleone, A. Giaconia, A.A. Lemonidou, State-of-the-art catalysts for CH_4 steam reforming at low temperature, Int. J. Hydrogen Energy 39 (2014) 1979–1997.
[12] A. Petersson, A. Wellinger, Biogas upgrading technologies–developments and innovations, IEA Bioenergy. (2009) 20.
[13] F. Bauer, C. Hulteberg, T. Persson, D. Tamm, Biogas upgrading- Review of commercial technologies, Swedish Gas Technol. Centre, SCG Rapp. 2013270. 270 (2013) 1–83.
[14] R. Augelletti, M. Conti, M.C. Annesini, Pressure swing adsorption for biogas upgrading. A new process configuration for the separation of biomethane and carbon dioxide, J. Clean. Prod. 140 (2017) 1390–1398.
[15] L.M. Robeson, The upper bound revisited, J. Memb. Sci. 320 (2008) 390–400.
[16] X.Y. Chen, H. Vinh-Thang, A.A. Ramirez, D. Rodrigue, S. Kaliaguine, Membrane gas separation technologies for biogas upgrading, RSC Adv. 5 (2015) 24399–24448.
[17] M.A. Llosa Tanco, D.A. Pacheco Tanaka, S.C. Rodrigues, M. Texeira, A. Mendes, Composite-alumina-carbon molecular sieve membranes prepared from novolac resin and boehmite. Part I: preparation, characterization and gas permeation studies, Int. J. Hydrogen Energy 40 (2015) 5653–5663.
[18] V. Spallina, D. Pandolfo, A. Battistella, M.C. Romano, M. Van Sint Annaland, F. Gallucci, Techno-economic assessment of membrane assisted fluidized bed reactors for pure H2 production with CO_2 capture, Energy Convers. Manage. 120 (2016) 257–273.
[19] K. Gerdes, W.M. Summers, J. Wimer, Cost Estimation Methodology for NETL Assessments of Power Plant Performance, Doe/Netl-2011/1455. (2011) 26.
[20] E. Rubin, G. Booras, J. Davison, C. Ekstrom, M. Matuszewski, S. McCoy, C. Short, Toward a common method of cost estimation for CO2 capture and storage at fossil fuel power plants, 2013.
[21] G. Manzolini, E. Macchi, M. Gazzani, CO_2 capture in natural gas combined cycle with SEWGS. Part B: economic assessment, Int. J. Greenh. Gas Control. 12 (2013) 502–509.
[22] DOE/NETL, Assessment of Hydrogen Production with CO2 Capture. Volume 1 : Baseline State-of- the-Art Plants, 2010.
[23] G. Manzolini, J.W. Dijkstra, E. Macchi, D. Jansen, Technical economic evaluation of a system for electricity production with CO_2 capture using a membrane reformer with permeate side combustion, Conf. Proc. ASME Turbo Expo. (2006) 1–11.
[24] W.D. Baasal, Preliminary Chemical Engineering Plant Design, Van Nostrand Reinhold, New York, 1990.
[25] S. Haider, A. Lindbråthen, M.-B. Hägg, Techno-economical evaluation of membrane

based biogas upgrading system: a comparison between polymeric membrane and carbon membrane technology, Green Energy Environ. 1 (2016) 222–234.
[26] H. Suda, K. Haraya, Gas permeation through micropores of carbon molecular sieve membranes derived from kapton polyimide, J. Phys. Chem. B 101 (1997) 3988–3994.
[27] A.B. Shelekhin, A.G. Dixon, Y.H. Ma, Theory of gas diffusion and permeation in inorganic molecular sieve membranes, AIChE J. 41 (1995) 58–67.